REMARKS

Applicants acknowledge receipt of the Office Action dated May 15, 2006, in which the Examiner objected to claims 5 and 47, rejected claim 47 under § 112, second paragraph, rejected claims 1-9 and 13-14 as anticipated by US 4865630 to Abe, and indicated that claims 10-12 would be allowable if rewritten in independent form.

Applicants respectfully traverse these rejections for the reasons set out below.

Status of the claims

Claims 1-14 are now pending.

Claims 15-47 have been cancelled.

Claim 48-52 are new.

Objection to claims 5 and 47

The Examiner asserts that "Claim 5 recites a method of making the permselective membrane, but fails to further limit . . . the membrane itself." Claim 5 requires that the permselective membrane be deposited by CVD. Applicants respectfully submit that this recitation does in fact limit the membrane. The recitation distinguishes CVD-deposited membranes from membranes deposited by other means, such as sol-gel techniques. As shown in the attached Exhibit A and Exhibit B (see highlighted passages), chemical vapor deposition (CVD) is different from sol-gel deposition and results in a different structure for the deposited layer. Thus, claim 5 does recite a further limitation over the recitation of claim 1. Applicants therefore respectfully request that this rejection be withdrawn.

The objection to claim 47 is moot, as claim 47 has been canceled.

Rejection of claim 47 under § 112, second paragraph

The rejection of claim 47 is also moot, as claim 47 has been canceled.

Rejection of claims 1-9 as anticipated by US 4865630 to Abe

Claim 1 has been amended to incorporate the limitation of claim 10, which was indicated to be allowable. Claim 1 is therefore now in condition for allowance, along with the claims that

depend from it.

Rejection of claims 13-14 as anticipated by US 4865630 to Abe

Claim 13 has been amended to incorporate the limitation of claim 10, which was indicated to be allowable. Claim 13 is therefore now in condition for allowance, along with claim 14, which depends from it.

Allowable Claims

Claim 10 has been cancelled and its limitation has been incorporated into claim 1. Claims 11-12, which formerly depended from claim 10, have been amended to depend from claim 1.

New claims

New claims 48-52, which depend from claim 1, have been added to recite the invention in further detail. The new claims do not include any new subject matter and are wholly supported by the specification as-filed.

Conclusion

Applicants believe that they have responded to all of the Examiner's objections and rejections and that the case is now in condition for allowance. If the Examiner has any questions or comments, or otherwise feels it would be advantageous, he is encouraged to telephone the undersigned at (713) 238-8043.

Respectfully submitted,

Marcella D. Watkins
Reg. No. 36,962
CONLEY ROSE, P.C.
P. O. Box 3267
Houston, Texas 77253-3267
(713) 238-8080
ATTORNEY FOR APPLICANT

Electrical Properties of YSZ Thin Films Deposited on Nanoporous Substrates

Yong-il Park, Yuji Saito, Rosana Pornprasertsuk, Jeremy Cheng, Suk-won Cha, Fritz B Prinz
Rapid Prototyping Laboratory, Department of Mechanical Engineering,
Stanford University, Stanford, CA94305, USA

ABSTRACT

Ultrathin YSZ(yttria stabilized zirconia) films having submicrometer thickness without gas leakage were successfully deposited on nanoporous alumina substrates for direct application to low-temperature SOFCs. By oxidation of metal thin films deposited onto anodic nanoporous alumina substrates with pore size of 20nm and 200nm using dc-magnetron sputtering at room temperature, aluminum oxide and YSZ thin films with thickness of about 30nm~300nm were obtained. During oxidation at high temperature the metal films were successfully transformed into defect-free oxide thin films and volume expansion induced from oxidation of metal resulted in dense thin films that are free from hydrogen permeation. Conductivity of YSZ thin films at room temperature was measured and compared with the reported conductivity of YSZ ceramics

INTRODUCTION

Gas-tight thin film deposition has been one of the key techniques in fields of gas sensors, gas-separating membranes and solid oxide fuel cells (SOFCs)

For now, a lot of effort has been dedicated to reducing electrolyte thickness which should result in a large decrease of ohmic resistance of the electrolyte layer and an expansion of working temperature region in fuel cell devices [1~4] One of the most conventional techniques for electrolyte layer fabrication is tape casting using slurry of micrometer-sized powders [1, 5] The resulting electrolyte membrane has high density, high mechanical strength and good electrical properties, but also has high ionic resistance due to its large thickness reaching several hundred micrometers. The second generation of SOFCs has anode-supported thin oxide films as their electrolyte membranes [4, 6~8]. The thickness of electrolyte layer could be reduced to 5μm~20μm and working temperature limit of fuel cell was also expanded from 800°C~1000°C to 500°C~1000°C.

Recently, high-tech processing such as PVD, CVD, PLD and sol-gel deposition has been tested to reduce electrolyte thickness and increase film density [1, 9~12] However, the oxide thin film deposition technologies that have been developed for decades are mainly for highly flattened substrates, especially silicon wafers [13~16], not for rough and porous substrates Since the electrolyte layer in SOFC should be deposited on porous electrodes to maintain high fuel-gas diffusion, it is not suitable to use the same deposition process for silicon wafers In general, electrolyte layer in solid oxide fuel cells should have the following properties: *i*) high ionic conductivity, *ii*) high density and uniformity to prevent potential drop by mixing of the fuel gases, *iii*) enough mechanical strength at high gas pressure, and *iv*) good adhesion to electrode layers without forming second phase to transfer ions. In spite of such difficulties, the need for a fuel cell working at intermediate temperature (200°C ~ 500°C) and thin film electrolyte membrane having submicron thickness has continuously arisen from industry [17]

There is an interesting report [18] about a successful deposition of continuous 'submicron' yttria stabilized zirconia (YSZ) thin films on anodic nanoporous alumina by sol-gel technique using viscous alkoxide-derived solution [18~20] Those substrates have highly ordered nanoholes

with uniform diameters, However, sol-gel derived thin films have several demerits, specifically, a large shrinkage during heat-treatment and low density from inherent high organic content that may cause local defects resulting in serious gas leakage. Therefore, these demerits may increase the attainable minimum film thickness needed to evade gas leakage.

In this paper, we demonstrate a simple but effective process for gas-tight YSZ thin film deposition on anodic nanoporous alumina substrates as a preliminary study of ultrathin electrolyte film deposition for low-temperature SOFCs. The key ideas are as follows:

i) Providing nanoporous alumina substrates with pore sizes varying from 20nm to 200nm to support electrolyte thin film.

ii) Depositing a metal film directly on the nanoporous alumina substrate in Ar atmosphere, and then oxidizing it at 400°C ~ 1000°C.

iii) The volume expansion of oxidized Y-Zr metal layer preventing gas leakage through thin films.

With these basic ideas, the possible procedure to enable ultrathin films to cover open pores and to work as a leak-free membrane is explained as shown in Fig. 1

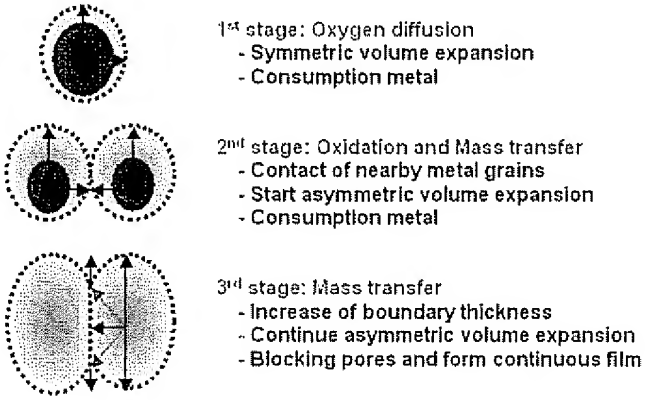

Fig. 1 Schematic diagram for the oxidation procedure of the thin film

By exposing atmosphere, diffusion of oxygen into the metal film starts. The surface reaction is generally fast in transition metals and changes the surface of metal forming an oxide layer even at room temperature, but further diffusion through the oxidized surface is different depending on materials. For example, aluminum has been known to make a protective oxide layer on the surface that strongly resists further oxygen diffusion [21], while other metals comprising elements for oxygen ionic conductors, but doped zirconia or doped ceria is easily oxidized in short time and at low temperature. By appropriate heat-treatment in oxygen atmosphere (or in air), oxygen diffuses through the surface to the inside of the metal layers resulting in volume expansion. The calculated volume expansion is 145.0% for zirconium metal (HCP, a=3.232Å, c=5.147Å) to cubic zirconia (FCC, a=5.139Å for composition having 15wt% of Y)[22]. Metal grains contact each other by the volume expansion covering open pores, and eventually forming gas-tight thin films through subsequent sintering. At this time, the stress formed by the collision of nearby grains attributes to asymmetric volume expansion mainly in the thickness direction. Therefore, the linear expansion of the cubic zirconia thin film can vary from 113.2% in symmetric expansion to 145% in asymmetric expansion in one direction. However, it is difficult to measure the exact thickness of the oxidized film, because the surface is quite rough and

thickness can vary by location, especially on top of the pores. During oxidation, mass transfer is also expected to occur as sintering increases film density and blocks macroscopic voids in thin films. Even though the nanoporous alumina substrate is an electronic insulator that cannot be used as an electrode for SOFC, there have been several reports about fabrication of functional substrates. That is, mesoporous YSZ and metal nanoporous replica from anodic alumina nanoporous substrates[12,19] that can be used as an nanostructured electrode-substrate for the thin films introduced in present study. Also other modifications to give appropriate electrical properties to the alumina substrate are also possible. The development of nanoporous substrate having the adequate electrical properties is another attractive theme to realize low-temperature SOFCs, and now is in progress by our group.

EXPERIMENTAL PROCEDURE

The materials used and experimental procedure (Fig. 2) are as follows. For nanoporous substrates, commercial inorganic alumina filters (Anodisc®, Whatman Inc.) with a pore size of 20nm and 200nm were used. The term 'pore size' used in this paper is defined by the producer with respect to their filtering ability, not by actual pore size. The observed actual pore diameters by SEM were 80nm ~ 200nm for 20nm-pore sized filters and 150nm ~ 300nm for 200nm-pore sized filters. The filter diameter (without support ring) was 40mm, filter thickness was 60μm and maximum working pressure was about 0.52MPa [23].

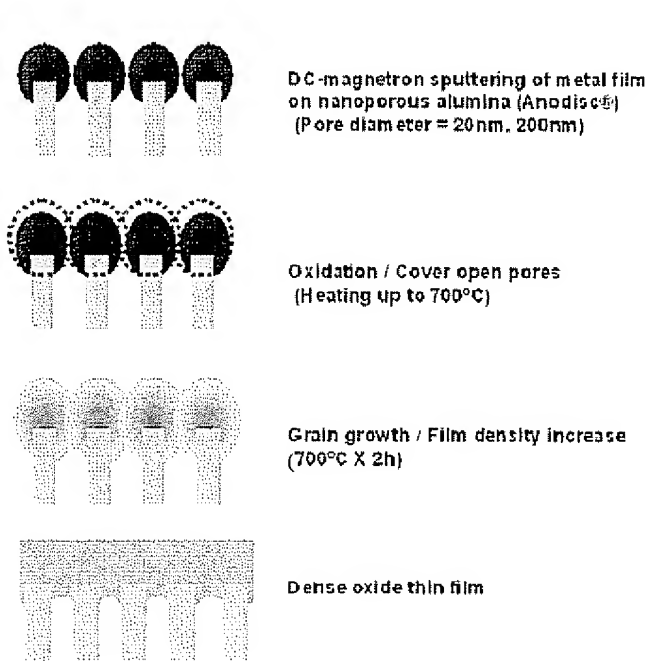

Fig. 2 Schematic drawing of the preparation of the ultrathin film fabrication on anodic porous alumina substrate

A Y-Zr complex target consisting of three or four 5mm×5mm×1mm-sized Y pellets with 99.9% purity on a Zr target with 99.7% purity was used for Y-Zr metal film deposition using DC-magnetron sputtering. The Ar gas flow rate was 10sccm ~ 30sccm and Ar pressure was 1.2Pa ~ 2.8Pa at 30W for Y-Zr deposition.

After deposition of metal film, subsequent oxidation was performed at 700°C for 2hours in air. Five YSZ thin films with three compositions of Y/Zr(at%) = 4/96, 16/84, 43/57 having different metal thickness from about 30nm~230nm were prepared. (Table 1)

Thickness of the films was controlled with the deposition rate, and was measured by using a Si wafer substrate with the same deposition condition.

The composition of Y/Zr was controlled by changing location and number of Y pellet. The Y/Zr composition was determined by X-ray photoemission spectroscopy (SSI S-Probe Monochromatized XPS Spectrometer)

Table 1 Prepared samples.

Sample		Pore size of substrate (nm)	Deposition condition (time(s) - Ar flow(Pa)-pressure(Pa) - energy(W))	As-sputtered thickness (nm)	Estimated thickness after oxidation (nm)		Observed thickness (nm)	Composition (at%)
					Symmetric expansion (ΔL=108.5% in Al =113.2% in Y-Zr)	Asymmetric expansion (ΔL=127.9% in Al =145.0% in Y-Zr)		
Al	A	20	32-10/1.2-50	30	32.6	38.6	~35	Al=99.999
	B	200	212-10/1.2-50	200	217.2	257.4	~240	
Y-Zr	C	20	400-10/1.2-50	38	43.0	55.1	~50	Y/Zr=3/97 (Y+Zr= >99.7)
	D	200						
	E	20	2000-10/1.2-50	190	215.1	275.5	~250	
	F	200						
	G	20	4000-30/2.5-20	-	-	-	-	Y/Zr=43/57 (Y+Zr= >99.7)
	H	20	4000-30/2.8-20	230	283.0	362.0	~320	Y/Zr=16/84 (Y+Zr= >99.7)

*All samples were finally oxidized at 700°C for 2hrs in air

The samples obtained were fixed with polymer adhesives on the top of thick silicone tubes connected to hydrogen cylinder, and then immersed in water to measure hydrogen permeance through oxidized thin films. The hydrogen pressure (ΔP) used for the permeance test was 0.1MPa. The microstructure of the thin films was observed with SEM, and phase development using sample A heat-treated at 400°C~1300°C for 2hours was observed using XRD.

Ionic conductivity of oxidized Y-Zr films was obtained from nyquist plots obtained using 0.03N NaCl-water solution as electrodes with Solartron 1260/1287 impedance analyzer at room temperature as shown in Fig. 3.

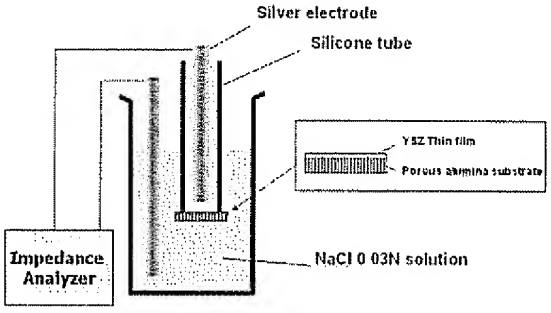

Fig. 3 Schematic drawing of the experimental setup for the resistance measurement

RESULTS AND DISCUSSION

1. Microstructure of YSZ Thin Films

In Fig. 4(a), SEM images of the surface of the as-deposited Y/Zr=4/96 metal film on substrate with 20nm-pores (Sample C in Table 1) are shown. All the pores of the substrate are perfectly closed by metal film, and a silver-colored smooth surface is observed despite the small thickness of only 50nm. Fig. 4(b) shows clear surface of oxide thin film (Sample E in Table 1) after oxidation at 700°C for 2h that is formed on porous substrate without any cracks and pinholes. Fig. 4(c) and (d) are for the surface and fractured edge of Y/Zr=16/84 film (Sample H in Table 1) oxidized at 700°C for 2h. The surface is not smooth and many large island-shaped grains are found. Although this sample showed good gas-separation, the rough surface should limit achievable minimum film thickness. The inhomogeneous surface could be due to the high Ar pressure to retain plasma on the complex target surface with the high contact resistance between Y-pellet and Zr target.

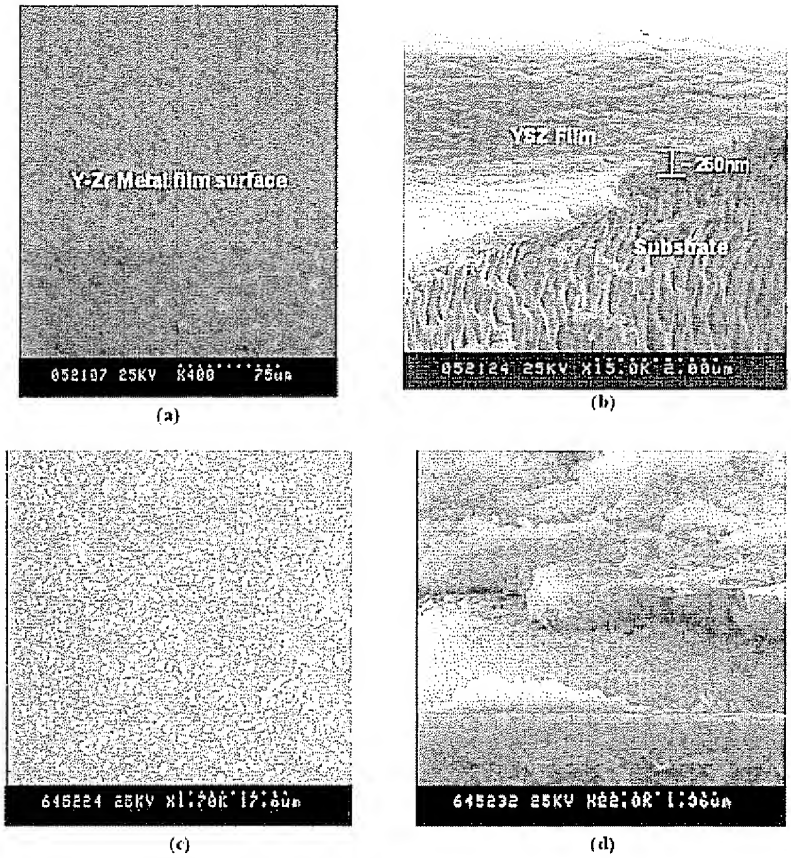

Fig. 9 SEM images of (a) surface of as-sputtered Y/Zr=4/96 metal film on substrate with 20nm-pores (Sample C in Table 1), (b) fractured edge of oxidized Y/Zr=4/96 film on substrate with 20nm-pores (Sample E in Table 1). (c) surface and (d) fractured edge of oxidized Y/Zr=16/84 film substrate with 20nm-pores (Sample H in Table 1)

2 Hydrogen Permeation Test of YSZ Thin Films

In Fig. 5, the measured hydrogen permeance for the oxidized Y-Zr thin films at 0.1MPa hydrogen pressure is illustrated. The permeance of the substrate without heating (Fig. 5(a), pore size=200nm; Fig 11(e), pore size=20nm) and with heating at 700°C for 2h (Fig. 5(b), pore size=200nm; Fig 11(f), pore size=20nm) are shown for comparison. The permeance for sample D (Fig 5(c)) slightly decreased to 7.49×10^{-7}mol/m^2·s·Pa. The value obtained shows the thin film does not have a good gas-separation property, but

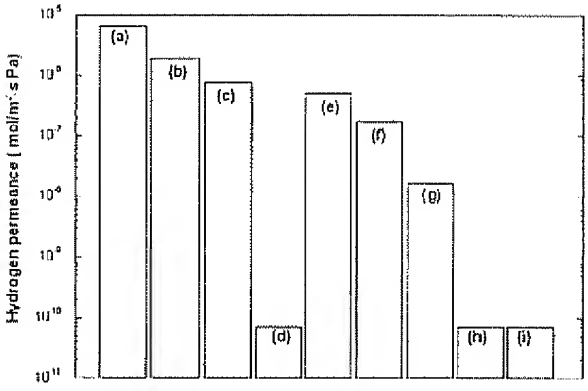

Fig. 11 Hydrogen permeance of the samples:
(a) substrate (pore diameter 200nm)
(b) substrate (pore diameter 200nm) after heat-treatment at 700°C for 2h
(c) sample D after heat-treatment at 700°C for 2h
(d) sample F after heat-treatment at 700°C for 2h
(e) substrate (pore diameter 20nm)
(f) substrate (pore diameter 20nm) after heat-treatment at 700°C for 2h
(g) sample C after heat-treatment at 700°C for 2h
(h) sample E after heat-treatment at 700°C for 2h
(i) sample G after heat-treatment at 700°C for 2h

the permeance for the sample C (Fig.5(d)) dropped to 7.44×10^{-11}mol/m^2·s·Pa, the measuring limit implying that the 250nm-thick film on 20nm-pore-sized substrate is enough to work as a gas separation layer. That is, the thickness of 50nm is not enough to cover 200nm-sized pores in the thin films deposited with current deposition condition that even results in rough and inhomogeneous surface as shown in Fig. 4(c). The permeances measured for the samples using the substrate with pore size of 20nm, Fig. 5(g), (h) and (i), show small permeance values, and the gas permeance for sample E and G (Fig. 5(h) and (i)) is very low and could not be detected with the present measurement settings (illustrated in Fig. 5 as 7.44×10^{-11}mol/m^2·s·Pa, the measuring limit value). Since the allowed limit for hydrogen permeance to start driving SOFC measured by our group is about 4.5×10^{-9}mol/m^2·s·Pa, the results obtained strongly support the high possibility for direct application to the low-temperature SOFCs.

It could be valuable to estimate how thin an oxide film is attainable at a fixed pressure difference(ΔP). The used sample can be simplified as a model shown in Fig. 6, and the minimum thickness is calculated by the following equations [24].

$$\sigma_{max} = 3/8 \cdot \{(1+\upsilon) \cdot (\Delta P \cdot R^2)\} / t^2 \quad \text{---------- } \textit{Eq. 1}$$

$$t = \sqrt{8/3 \cdot \sigma_{max} / \{(1+\upsilon) \cdot \Delta P \cdot R^2\}} \quad \text{---------- } \textit{Eq. 2}$$

where, σ_{max} : Ultimate tensile strength
ΔP : Pressure difference
υ : Poisson's ratio
R : Pore radius
t : Film thickness

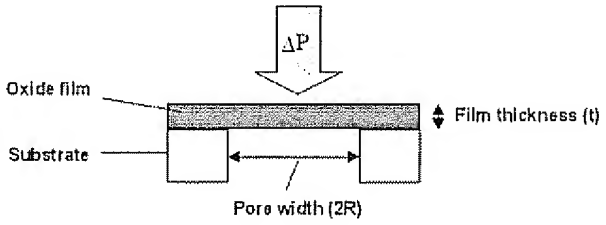

Fig. 6 Simplified model of the samples.

The attainable minimum film thickness for 8YSZ thin films on the porous substrate (pore size: 20nm , ΔP: 0.1MPa) estimated with the model shown in Fig. 6, *Eq-2*, and the reported mechanical properties of 8YSZ sheet [25] is 6.61nm at room temperature.

However, there are too many differences between bulk ceramics and thin films to directly apply the values reported for bulk alumina to this estimation. Considering the difference in grain size, density, impurity, and defects, especially pore diameter and distribution which critically affect fracture strength, the reasonable minimum thickness might be larger than the estimation. Of course, the difference between the reported mechanical data for 8YSZ sheet and thin films also should be noted, and therefore the reasonable minimum thickness might be larger than the estimation.

Nevertheless, the estimated thickness limit is still important as a milestone for further study.

3. Oxidation and Phase Development of YSZ Thin Films

To observe phase development after oxidation of the Y-Zr thin films, XRD patterns obtained with sample C are illustrated in Fig. 7. There is no distinct crystalline peak in the pattern at room temperature (Fig. 7(c)) and at 500°C (Fig. 7(d)) for sample E, the Y/Zr=3/97 thin film. However, the color of thin film changed from metal silver to glassy transparent during oxidation at 500°C for 10h. At 700°C, a clear crystalline phase is detected. As mentioned above, the crystalline phase for Y-Zr film is easily achieved at a lower temperature than alumina thin film due to its inherent high oxygen diffusivity. The observed crystalline peaks match a mixed phase of cubic and monoclinic (Fig. 7(e)) that has been reported as a crystalline phase for a solid solution of Y_2O_3 and ZrO_2 having a composition in the range of about 3/97 ~ 15.6/83.4 of Y/Zr composition [26]. By increasing the yttrium concentration from 3at%(sample E, Fig. 7(e)) to 16at%(sample H, Fig. 7(f)) and 43at%(sample G, Fig. 7(g)), the monoclinic phase in oxidized thin film disappears and clear cubic single phase is achieved.

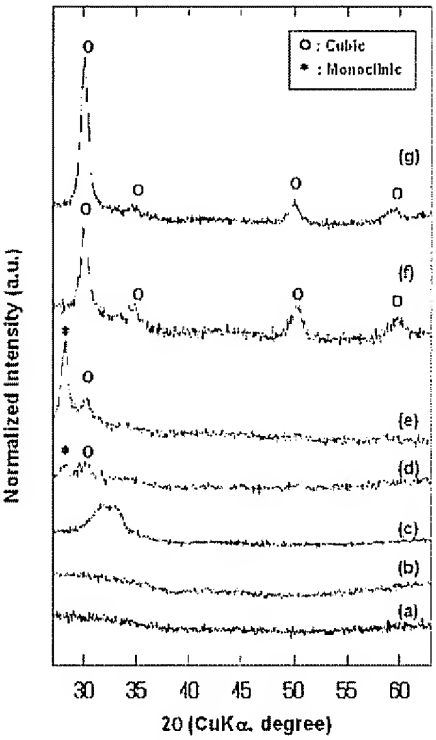

Fig. 12. XRD patterns for YSZ thin films and substrates (Y/Zr denotes atomic percent of Y and Zr in thin films)
(a)substrate at room temperature,
(b)substrate heat-treated at 700°C for 2h,
(c)as-sputtered sample E, Y/Zr=3/97 metal thin film on substrate (room temperature),
(d)sample E, oxidized Y/Zr=3/97 film at 500°C for 10h
(e)sample E, oxidized Y/Zr=3/97 film at 700°C for 2h,
(f)sample H, oxidized Y/Zr=16/84 film at 700°C for 2h
(g)sample G, oxidized Y/Zr=43/57 film at 700°C for 2h.

The relative intensity estimated from the fitted peaks, that is, (111), (200), (220), and (311), matched well with the relative peak intensity from the reported data for the bulk polycrystalline $Y_{0.15}Zr_{0.85}O_{1.93}$ indicating that the film has no preferred orientation (Table 2).

To define if the thin film has c-axis orientation, the Lotgerling's orientation factor(F) was checked using the following equations (*Eq. 3 and 4*).

$$F = (f - f_0) / (1 - f_0) \quad \text{-------} \textit{Eq. 3}$$

$$f = \Sigma I(00l) / \Sigma I(hkl) \text{ -------} \textit{Eq. 4}$$

where, I = peak intensity
f_0 = f from reference data

The estimated F is 0.001, indicating the obtained thin film has no preferred orientation.

The crystalline YSZ could be easily obtained by oxidation at 500°C ~ 700°C, a quite lower temperature than alumina thin film. It is noteworthy that the oxidation of oxygen-conducting oxide thin films from their metal states occurs at very low temperatures with high speed. Therefore, the suggested process also has a role as a low-temperature processing for oxide thin

films, not to mention as an ultra-thin film processing having nano-size effect on electrical properties.

Table 3 The relative peak intensities from the reference data and from the measured YSZ peaks.

Miller indices	Reference		Measured	
	Intensity (I_0)	Relative Intensity ($I_0 \times 100 / \Sigma I_0$)	Intensity (I)	Relative Intensity ($I \times 100 / \Sigma I$)
(111)	100	45.5	2086.1	51.5
(200)	25	11.4	404.3	10.0
(220)	55	25.0	969.2	23.9
(311)	40	18.2	588.3	14.53

4 Conductivity of YSZ Thin Films

In Fig. 8, the obtained Nyquist plots for sample E ((a) ○, Y/Zr=3/97, thickness: 250nm), sample C ((b) ■, Y/Zr=3/97, thickness: 50nm) and sample H ((c) △, Y/Zr=16/84, thickness: 320nm) are shown. The obtained obvious semicircles represent resistance of the YSZ thin films on porous substrates, and a small resistance component by the electrode-solution is also found. About 6000Ω of resistance at the left ends of the semicircles matched well with the measured electrode resistance of 0.03N-NaCl. As the thickness is reduced from 250nm(sample E) to 50nm(sample C), the resistance decreases from $3.67\times10^{8}\Omega$ (Fig. 8(a)) to $2.50\times10^{7}\Omega$ (Fig. 8(b)).

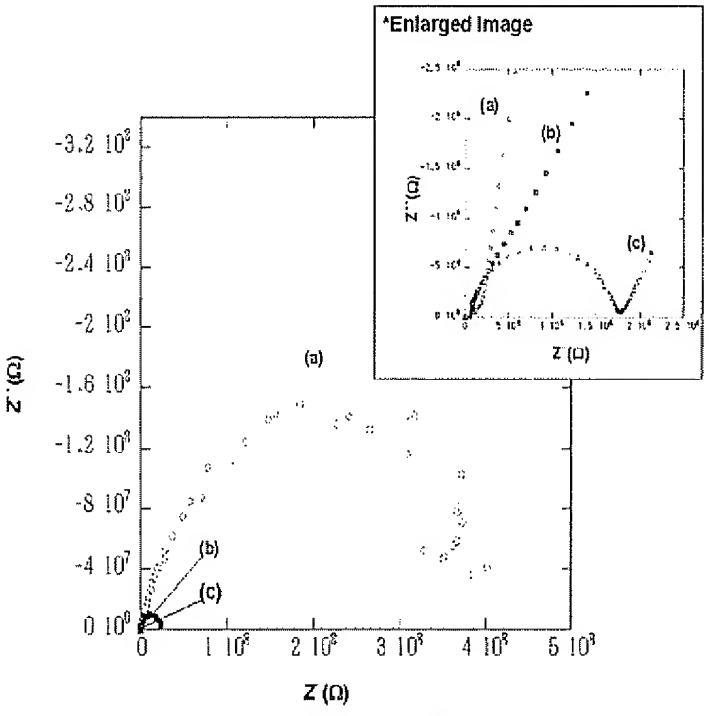

Fig. 14 Nyquist plots for (a)sample E (○), (b)sample C (■) and (c)sample H (△) (see Table 1 for definition of the samples)

A large decrease of resistance to $1.79\times10^{5}\Omega$ (sample H, Fig. 8(c)) was observed by changing composition from Y/Zr=3/97 to Y/Zr=16/84 in spite of the film thickness being thicker (~320nm) than the other two samples.

The conductivity for samples E and C, which have the same composition (Y/Zr=3/97) and different thickness (50nm and 250nm), calculated from the resistances obtained from the nyquist plots (Fig. 8(b) and (c)) are 4.07×10^{-12}S/cm and 1.11×10^{-12}S/cm respectively, showing almost the same value. However, the conductivity for sample H (Fig. 8(a)) with a composition of increased yttrium concentration (Y/Zr=16/84) showed a much higher value of 3.42×10^{-9}S/cm.

SUMMARY

A fabrication of ultrathin YSZ films without gas leakage was investigated for low-temperature SOFCs application. To obtain polycrystalline YSZ thin films with submicron thickness, Y-Zr metal thin films were deposited onto anodic nanoporous alumina substrates with pore sizes of 20nm and 200nm using dc-magnetron sputtering at room temperature. By subsequent oxidation at high temperature over 500°C, the metal films were successfully transformed into oxide thin films. Volume expansion induced from oxidation of metal resulted in dense thin films that were free from hydrogen permeation, even though the thickness was as thin as about 30nm~300nm. Conductivity of 8YSZ(Y/Zr=16/84) thin film at room temperature was 3.42×10^{-9}S/cm.

REFERENCES

1. J. Will, A. Mitterdorfer, C. Kleinlogel, D. Perednis, L. J. Gaukler, *Solid State Ionics*, **131**, 79-96 (2000).
2. Y. Jiang, A. V. Virkar, *J. Electrochem. Soc.*, **148**, 7, A706-A709 (2001).
3. B. Zhu, *J. Power Sourc.*, **93**, 82-86 (2001).
4. R. Doshi, V. L. Richards, J. D. Carter, X. Wang, M. Krumpelt, *J. Electrochem. Soc.*, **146**, 4, 1273-1278 (1999).
5. B. H. Rabin, *J. Am. Ceram. Soc.*, **73**, 2757 (1990).
6. B. C. H. Steele, *Solid State Ionics*, **134**, 3-20 (2000).
7. Y. Jiang, A. V. Virkar, *J. Electrochem. Soc.*, **148**, 7, A706-A709 (2001).
8. J. Schoonman, J. P. Dekker, J. W. Briers, N. J. Kiwiet, *Solid State Ionics*, **466**, 299 (1991).
9. L. S. Wang, S. A. Barnett, *Solid State Ionics*, **61**, 273-276 (1993).
10. A. F. Jankowski, J. P. Hayes, *Surf. Coat. Technol*, **76-77**, 126-131, (1995).
11. C. Xia, S. Zha, W. Yang, R. Peng, D. Peng, G. Meng, *Solid State Ionics*, **133**, 287-294 (2000).
12. X. Changrong, C. Huaqiang, W. Hong, Y. Pinghua, M. Guangyao, P. Dingkun, *J. Membrane Sci.*, **162**, 181-188 (1999).
13. G. Koren, E. Polturak, B. Fisher, D. Cohen and G. Kimel, *Appl. Phys. Lett.*, **53**, 2330 (1998).
14. N. Wakiya, T. Yamada, K. Shinozaki, N. Mizutani, *Thin Solid Films*, **371**, 211-217 (2000).
15. S. Horita, H. Nakajima, T. Kuniya, *Vacuum*, **59**, 390-396 (2000).
16. M. Hartmanova, K. Gmukova, M. Jergel, I. Thurzo, F. Kundracik, M. Brunel, *Solid State Ionics*, **119**, 85-90 (1999).
17. J. Van herle, R. Ihringer, N. M. Sammes, G. Tompsett, K. Kendall, K. Yamada, C. Wen, T. Kawada, M. Ihara, J. Mizusaki, *Solid State Ionics*, **132**, 333-342 (2000).
18. Timothy W. Kueper, Steven J. Visco and L. C. De Jonghe, *Solid State Ionics*, **52**, 251-259 (1992).
19. H. Masuda, K. Hukuda, *Science*, **268**, 1466-1468 (1995).
20. H. Masuda, F. Hasegawa, S. Ono, *J. Electrochem. Soc.*, **144**, 5 (1997).
21. H. Bolt, F. Koch, J. L. Rodet, D. Karpov, S. Menzel, *Surf. Coat. Technol.*, **116-119**, 956-962 (1999).
22. JCPDS-ICDD file, Nos. 30-1468.
23. http://www.whatman plc.uk/products/analytical/labfiltration/a_pd_labfil_013.html
24. M. F. Ashby, *Materials Selection in Mechanical Design*, Butterworth-Heinmann, Oxford, 1996.
25. A. Atkinson, A. Selçuk, *Solid State Ionics*, **134**, 59-66 (2000).
26. H. G. Scott, *J. Mater. Sci.*, **10**, 1527-1535 (1975).

Smithsonian/NASA ADS Physics Abstract Service

· **Find Similar Abstracts (with default settings below)**
· **Also-Read Articles** (Reads History)

· **Translate Abstract**

Title:	Synthesis of Indium Tin Oxide Thin Films by Cvd and Sol-Gel Processing.
Authors:	Bernard, Laurent-Sebastien
Affiliation:	POLYTECHNIC UNIVERSITY.
Publication:	Thesis (PH.D.)--POLYTECHNIC UNIVERSITY, 1994.Source: Dissertation Abstracts International, Volume: 54-11, Section: B, page: 5650.
Publication Date:	00/1994
Category:	Chemistry: Inorganic; Physics: Condensed Matter; Engineering: Materials Science
Origin:	UMI
Abstract Copyright:	(c) 1994: UMI Company
Bibliographic Code:	1994PhDT.....63B

Abstract

The object of this work was to synthesize indium tin oxide thin films on glass substrates using Chemical Vapor Deposition and Sol-gel processes. Starting materials included indium-2,2,6,6-tetramethylheptane - 3,5-dione and tin chloride as precursors for the CVD method, indium nitrates (In(NO_3)_35H _2O), tin chloride and ethylene glycol for the sol-gel method. A spin coating system was used to prepare the films by sol-gel. Analyses were carried out by X-ray powder diffraction, scanning electron microscope (SEM), four probe resistivity measurements, profilometry, atomic absorption and Hall effect measurements. Continuous, adherent films with high visible optical transmission and low resistivities were obtained at a deposition temperature of about 500 ^circC. A pressure of 1.5 torr was used for the CVD technique. Films made by a sol-gel technique were annealed under vacuum (6 times 10^{-2} torr) in order to obtain low resistivity. The films obtained by the CVD process exhibited lower resistivity and better optical transmission. Some of the differences between the films made by CVD and sol-gel have been explained in term of grain sizes. Larger grain size for the CVD films, leading to lower resistivity, were due to the growth process.

Bibtex entry for this abstract **Preferred format for this abstract** (see Preferences)

Add this article to private library | Remove this article from private library

---

Find Similar Abstracts:

Use: ☐ Authors